LIMNOLOGY and OCEANOGRAPHY

ASLO

Limnol. Oceanogr. 69, 2024, 712–722

doi: 10.1002/lno.12535

Light-use efficiency for coral reef communities and benthic functional types

Eric J. Hochberg,[1*] **Chiara Pisapia**,[2] **Robert C. Carpenter**,[3] **Siarah Hall**[4]

[1]Bermuda Institute of Ocean Sciences, Arizona State University, St. George's, Bermuda
[2]King Abdullah University of Science and Technology, Thuwal, Saudi Arabia
[3]Department of Biology, California State University, Northridge, California, USA
[4]Florida Fish and Wildlife Conservation Commission, St. Petersburg, Florida, USA

Abstract

Coral reef metabolism is dominated by benthic photoautotrophic communities that comprise varying combinations of algae, coral, and sand. Rates of daily gross primary production (GPP) for these benthic functional types (BFTs) are remarkably consistent across biogeographical regions, supporting the idea that reefs exhibit modal metabolism. Most variability in reported rates likely arises from differences in light availability. In fact, GPP is a linear function of incident photosynthetically active radiation (PAR), the fraction of PAR absorbed (fAPAR) by photoautotrophic organisms or communities, and light-use efficiency (ε), which parameterizes photosynthesizers' biochemical capacity for CO_2 fixation: GPP $= \varepsilon \times$ fAPAR $\times$ PAR. On time scales of days to weeks, fAPAR and ε are far more stable than PAR. ε is a critical parameter, because it represents productive response integrated across all environmental conditions, other than light. If BFTs exhibit consistent GPP across wide geographic ranges, then their εs must also be consistent. The aim of this study was to estimate ε for algae, coral, and sand. Using data collected during NASA's CORAL mission in 2016–2017, ε was calculated for 32 mixed communities at Lizard Island, Australia (10); Kāne'ohe Bay, Hawai'i (8); Guam (6); and Palau (8). Nonnegative least squares was used to solve for ε of each BFT, producing values of 0.038, 0.060, and 0.016 C photon^{-1} for algae, coral, and sand, respectively. These values can be used in light-driven models of reef metabolism. Further work is necessary to refine these estimates and, importantly, to explore how ε is affected by environmental conditions.

Knowledge of coral reef daily gross primary production (GPP) is the foundation for understanding reef system function (Odum and Odum 1955). GPP sets the maximum energy available to a reef community through autotrophic pathways and ultimately limits the biomass and secondary production of reef consumers (Atkinson and Grigg 1984; Grigg et al. 1984; Polovina 1984). Respiration (R) nearly balances GPP, so that daily (and longer) net primary production (NPP) is typically very small (Kinsey 1985; Falter et al. 2011), but anomalous rates for NPP and GPP can be useful diagnostic indicators of reef trophic status. Calcification (G) is the net gain of biogenically derived carbonates, which determines the long-term growth of the reef structure (Kinsey 1985). G is directly related to the value of GPP (Chalker 1981; Barnes and Devereux 1984; Gattuso et al. 1999; Atkinson and Falter 2003). GPP/R/NPP and G represent the organic and inorganic growth of reefs, and they are arguably the most basic and most important reef ecosystem functions. Because GPP drives R and NPP (Falter et al. 2011), as well as G (Gattuso et al. 1999), understanding the impacts of global change on reef ecosystems cannot be complete without knowledge of trends and dynamics of GPP.

Historically, in situ measurements of reef metabolism have relied on smaller-scale (1s of m^2) benthic enclosures (Kinsey 1978; Yates and Halley 2003) or larger-scale (100s–1000s of m^2) flow respirometry (Marsh and Smith 1978; Falter

*Correspondence: ejhochberg@bios.asu.edu

Additional Supporting Information may be found in the online version of this article.

Author Contribution Statement: EJH: Conceptualization; formal analysis (lead); funding acquisition; investigation (equal); methodology (equal); project administration (lead); resources (equal); visualization; writing—original draft preparation; writing—review and editing (lead). CP: Formal analysis (supporting); investigation (equal); methodology (equal); writing—review and editing (supporting). RC: Conceptualization (supporting); investigation (equal); methodology (equal); project administration (supporting); resources (equal); writing—review and editing (supporting). SH: Formal analysis (supporting); writing—review and editing (supporting).

et al. 2008). Recent application of boundary layer methods, such as gradient flux (McGillis et al. 2011) and eddy correlation (Long et al. 2013), has afforded researchers the ability to measure productivity under conditions of natural water flow at intermediate, community-level scales (10s to 100s of m^2) and in a wider array of environments than previously possible with Lagrangian or Eulerian techniques (Falter et al. 2008).

Combined, these approaches have revealed some important general trends. Reef metabolism is apparently tri-modal, with high-biomass, three-dimensional benthic communities such as coral thickets and knolls having the highest GPP at 1–2 mol C m^{-2} d^{-1}; algal dominated areas have rates about half that at 0.5–1 mol C m^{-2} d^{-1}; and sandy and rubble areas have rates about an order of magnitude lower at 0.1–0.2 mol C m^{-2} d^{-1} (Kinsey 1985; Pisapia et al. 2021). In summarizing the early research into reef biogeochemistry, Kinsey (1983, 1985) posited that, because of these modal rates, coral, algae, and sand represent fundamental benthic functional types (BFTs). It follows that changes in the coral : algae : sand ratio therefore can result in substantial changes to ecosystem function, as suggested by Odum and Odum (1955).

The spatial arrangement of these BFTs describes the fundamental zonation of a reef, which can be interpreted as a measure reef status. Healthy reefs exhibit high GPP on fore-reefs, reef-crests, and reef-flats, leading to net autotrophy (GPP/R > 1). Active sand burial in back-reef areas leads to low GPP and net heterotrophy (GPP/R < 1; Kinsey 1979; Hatcher 1990; Atkinson and Falter 2003). Kinsey (1985) has noted that reef-flat communities typically have low topographical relief and are usually a mixture of coral, algae, and sand, with GPP of 0.3–1.6 mol C m^{-2} d^{-1} (Kinsey's "standard" GPP is 0.6 mol C m^{-2} d^{-1}). While this overall zonation has been a convenient pattern to evaluate reefs, there are many variations.

Falter et al. (2008, 2011) have made daily observations of reef productivity for up to $\sim$2.5 weeks. Their results demonstrate tight coupling between GPP and R, which indicates that most fixed carbon is rapidly respired within the autotrophs (Falter et al. 2011). There is typically strong seasonality in GPP (and R), with summer values $\sim 2\times$ those of winter (Kinsey 1985; Gattuso et al. 1999). However, the strength of that effect is inversely proportional to latitude (Kinsey 1985). Thus, while irradiance should play a central role, there must also be a confounding effect due to temperature and/or other climate variables.

Despite its importance, there seems to have been little effort devoted toward studying changes in GPP specifically to evaluate trajectories of reef ecosystems (Atkinson and Cuet 2008). One reason scientists have not addressed this task might be that traditional in situ measurements of reef metabolism are logistically unwieldy. The flow respirometry approach is confined to shallow reef-flats under limited environmental conditions, and it relies on integration over large reef areas that incorporate multiple BFTs. The benthic enclosure approach allows rate measurements for discrete BFTs, but enclosure deployment is cumbersome, and measurements are few. The boundary layer approaches theoretically enable flowing-water measurements in any reef environment, but they have high associated costs and are cumbersome for areally extensive measurements (Takeshita et al. 2016, 2018).

Another reason that reef status assessments do not include GPP is the inherent difficulty interpreting measured values. Notwithstanding Kinsey's concept of modal rates and a metabolic standard for reef flats, values of GPP can be highly variable between reefs, as well as for a single reef from one day to the next. The largest driver of this variability is changing irradiance (Kinsey 1985; Gattuso et al. 1999; Atkinson and Falter 2003). Falter et al. (2011) have leveraged this light-driven variability to demonstrate very nicely the strong short-term coherency between GPP and R by measuring the two rates for the same reef community over a period of sunny days immediately followed by a period of cloudy days. However, it is equally clear that, when assessing reef status, the widely different values of GPP measured on sunny vs. cloudy days do not indicate rapid shifts in benthic community structure or reef function.

A census-based approach can be applied to extrapolate respirometry-derived productivity values across whole-reef systems. First, rates are determined for each basic community-type or habitat present on the reef, either measured in situ (Atkinson and Grigg 1984; Brock et al. 2006) or taken from the literature (Andréfouët and Payri 2000). Then, the total coverage of each community-type or habitat is estimated, either through in situ surveys (Courtney et al. 2016) or remote sensing (Atkinson and Grigg 1984; Andréfouët and Payri 2000; Brock et al. 2006). Finally, the average rate for each community is multiplied by the community's total area, and the products are summed across all community types to give an estimate for system-scale primary production. Given a map of benthic types, as from remote sensing, rates can be applied on a pixel-by-pixel basis, generating a map of spatially distributed estimated productivity (Andréfouët and Payri 2000; Brock et al. 2006; Moses et al. 2009). This approach has proven useful for describing the general distribution of metabolism on reefs, but it is ultimately limited because it does not allow for variable rates within community types, and it does not allow for variable community/habitat composition. Importantly, the census-based approach does not (at present) accommodate variable light intensity.

Following an approach that is well developed in terrestrial ecology, and somewhat less well-developed for oceanic systems, Hochberg and Atkinson (2008) proposed an optical absorptance-based method for estimating reef community-scale GPP. The basic concept is to account for all quanta absorbed by the benthos, then apply an appropriate community light-use efficiency (ε, C fixed or O_2 evolved per quanta absorbed), thus deriving photosynthetic rates.

Hochberg and Atkinson (2008) pointed out that there are no published values describing ε at the reef benthic community scale or for reef BFTs, which remains true as of mid-2023.

The authors surveyed the literature to compile initial slopes of organism-scale photosynthesis–irradiance curves (Chalker 1981) for various coral and algae types. They found a mean value across all benthic types of 0.0328 C photon^{-1}, with wide variability (SD 0.0189 C photon^{-1}). The compiled data did suggest that organism-scale ε may vary between BFTs and with environmental conditions, but the volume of data was insufficient to determine significant trends. Variability in ε should be expected at the community scale, but it is probably (much) less than that reported for the organism scale. Reef benthic communities are inherently mixed with 10s to 100s of different photosynthetic taxa. Thus, ε should converge to a few, fairly stable values, depending on the BFTs.

During 2016–2017, the NASA Earth Venture Suborbital-2 mission COral Reef Airborne Laboratory (CORAL) visited the Great Barrier Reef, Hawai'i, Mariana Islands, and Palau. In support of the hyperspectral remote sensing map products, CORAL conducted extensive in-water validation activities, including measurements of community GPP, photosynthetically active radiation (PAR), and benthic cover (BC) (Pisapia et al. 2021). The aim of the present study is to use the CORAL data to make the first-ever estimates of ε for reef communities. The specific objectives are (1) to estimate community-scale ε for each suitable CORAL validation site, and (2) to derive ε for each of the fundamental BFTs (algae, coral, sand).

Methods

Background

The light-use efficiency model for GPP is

$$\mathrm{GPP} = \varepsilon \times \mathrm{APAR} = \varepsilon \times \mathrm{fAPAR} \times \mathrm{PAR} \tag{1}$$

where PAR is incident photosynthetically active radiation (quanta m^{-2} d^{-1}), fAPAR is the fraction of PAR absorbed by the photosynthetic organism or community (0…1), and APAR = fAPAR × PAR is the total absorbed PAR (quanta m^{-2} d^{-1}). This is the general form of primary production models that are based on light-use efficiency, first suggested by Monteith (1972, 1977). This type of model is now routinely used in terrestrial remote sensing studies (e.g., Running et al. 2004; Fensholt et al. 2006; Sims et al. 2006) and forms the basis for standard MODIS global land GPP and NPP products (Heinsch et al. 2003). Similar expressions have also been utilized with respect to marine systems (Morel 1978; Platt 1986; Attard and Glud 2020), including corals (Wyman et al. 1987). Through a modeling study, Sawall and Hochberg (2018) have demonstrated the applicability of this linear model of time-integrated productivity for corals and reef communities.

In conceptual terms, fAPAR expresses the factors that determine light absorption, mostly photosynthetic pigment concentrations and the three-dimensional structure of the plant/community (Gitelson and Gamon 2015). In contrast, ε is the expression of physiological response to environmental conditions and ontogenetic status (Field 1991). Under stress conditions (e.g., temperature or nutrient), plant/community ε is reduced from a theoretical $\varepsilon_{\max}$ (efficiency under ideal conditions). It is important to reiterate that Eq. (1) applies to time-integrated rates. Thus, ε does not directly represent instantaneous photosynthetic reactions, but their cumulative result at the day scale (or longer).

Operationally, the main utility of Eq. (1) is that, given knowledge of ε, determination of GPP relies only on straightforward optical measurements, as opposed laborious and/or expensive Lagrangian, Eulerian, or boundary layer observations. Eq. (1) also operates at any scale for which ε can be defined, typically the organism or community, but potentially even an entire ecosystem (Field 1991). Finally, rearranging Eq. (1), it is clear that ε represents GPP normalized by APAR:

$$\varepsilon = \mathrm{GPP} \div \mathrm{APAR} = \mathrm{GPP} \div (\mathrm{fAPAR} \times \mathrm{PAR}). \tag{2}$$

This normalization removes the wide variability in GPP engendered by variable light capture. This enables more direct comparison between different communities/reefs or between time points for the same community/reef. Any variation in ε is not due to light, but some other impact on productive status.

Assuming that GPP is an additive ecosystem function (Hatcher 1997), a reef community comprising various amounts of algae, coral, and sand would have a total rate equaling the sum of the three BFTs:

$$\mathrm{GPP}_{\mathrm{community}} = \mathrm{GPP}_{\mathrm{algae}} + \mathrm{GPP}_{\mathrm{coral}} + \mathrm{GPP}_{\mathrm{sand}} \tag{3a}$$

In the framework of Kinsey's modal rates, each mode is weighted by its contribution to the community:

$$\mathrm{GPP}_{\mathrm{community}} = \sum \mathrm{BC}_i \times \overline{\mathrm{GPP}}_i \tag{3b}$$

where i = (algae, coral, sand) is the set of BFTs, $\overline{\mathrm{GPP}}$ is the modal (or average) rate, and BC is proportional BC for the given BFT. Eq. (3b) is the census-based model for GPP.

Equation (1) can be placed in a census-based framework by partitioning ε and fAPAR as their weighted means with respect to the BFTs, as

$$\mathrm{GPP}_{\mathrm{community}} = \sum (\mathrm{BC}_i \times \varepsilon_i) \times \sum (\mathrm{BC}_i \times \mathrm{fAPAR}_i) \times \mathrm{PAR} \tag{4}$$

This is a highly flexible model, allowing for variable light intensity (PAR), variable light capture (fAPAR$_i$), and variable light-to-carbon conversion efficiency (ε_i). Parameterizing Eqs. (1) and (4) is mostly straightforward. PAR and BC are readily and routinely measured on coral reefs. Measuring fAPAR is not difficult (e.g., Hochberg et al. 2003), though it is rarely performed, if ever. It is ε that requires most attention.

Study sites and measuring GPP

CORAL validation campaigns were conducted during late winter/spring at Lizard Island, Queensland, Australia (September 2016); Kāne'ohe Bay, Hawai'i (February 2017); Guam (April 2017); and Palau (May 2017). Within each locale, the gradient flux method (McGillis et al. 2011) was deployed to measure GPP (mol C m^{-2} d^{-1}) over a full diurnal cycle at several sites (Fig. 1). Details of deployments and calculations are in Pisapia et al. (2021). GPP varied with BC, but not with geographic location, enabling the present analysis that ignores location.

Measuring BC

At each GPP site, divers collected ~ 1000 overlapping underwater photographs covering an area ~ 10 m $\times$ 10 m, centered on the gradient flux mooring. The photographs were collected in RAW format using a combination of Nikon D5500 and Canon EOS 7D Mark II cameras. Color temperature and exposure of the RAW images were adjusted in Adobe Camera Raw to obtain relatively even balance between the blue, green, and red channels. The adjusted photographs were saved in JPEG format at maximum quality. Agisoft PhotoScan Pro (now Metashape Pro) was used to stitch the photographs together into a single, large orthomosaic. BC was determined by overlaying 100 points on the orthomosaic in a 10×10 grid, then identifying the organism or substrate under each point to the lowest possible taxonomic level. For the purposes of this study, identifications were simplified to the BFTs algae, coral, or sand. BC was determined by dividing the number of points identified as a given BFT by the total number of points.

Measuring PAR

A cosine irradiance sensor (Biospherical Instruments QCP-2150) was deployed in conjunction with the GPP measurements during the CORAL validation campaigns. The sensor measured downwelling plane irradiance with a PAR response at one-minute intervals for the duration of each campaign. In some instances, the sensor was mounted directly on the base of the gradient flux mooring. In other instances, the sensor was moored nearby, but possibly at a different depth. To correct PAR for the depth difference, the following relation was used (Maritorena et al. 1994):

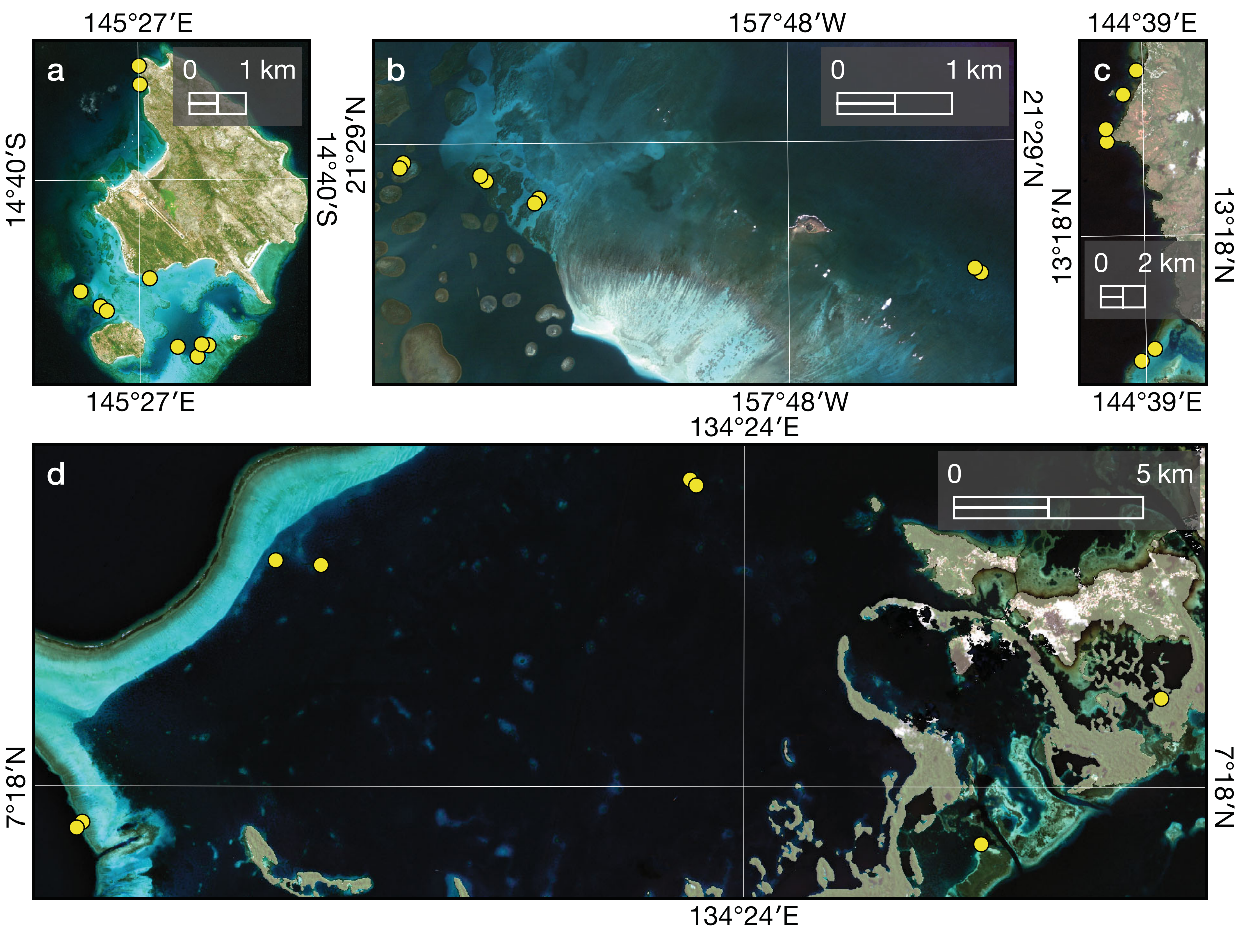

Fig. 1. Maps of CORAL campaigns showing gradient flux sites. (**a**) Lizard Island, GBR (September 2016). (**b**) Kāne'ohe Bay, Hawai'i (February 2017). (**c**) Guam (April 2017). (**d**) Palau (May 2017). Satellite basemaps from Sentinel-2 L2A data products.

$$\mathrm{PAR}(z_2) = \mathrm{PAR}(z_1) \times \exp[-K_\mathrm{d}(\mathrm{PAR}) \times (z_2 - z_1)] \quad (5)$$

where z_1 is the depth of the sensor, z_2 is the depth of the seafloor at the gradient flux mooring, and K_d(PAR) is the diffuse attenuation coefficient for downward PAR. Depths were measured at time of deployment via scuba. K_d(PAR) was estimated as the average value for reef waters from Hochberg et al. (2020).

Modeling fAPAR

fAPAR was not measured during the CORAL field validation campaigns and therefore was estimated via modeling for this study, based on the relation fAPAR = APAR ÷ PAR (*see* Eq. 1). Here, both APAR and PAR were modeled to ensure proper scaling between the two.

First, to obtain modeled PAR, spectral irradiance just below the sea surface [$E_d(\lambda;0^-)$, where $\lambda = 400$–700 nm] was modeled (Gregg and Carder 1990), then propagated to depth (H) of the given site following $E_d(\lambda;H) = E_d(\lambda;0^-) \times \exp[-K_d(\lambda) \times H]$. Average reef $K_d(\lambda)$ from Hochberg et al. (2020) was used. PAR for this arbitrary (realistic, but not real) condition was determined as $\int E_d(\lambda;H)\,\mathrm{d}\lambda$.

Next, a spectral reflectance [$R(\lambda)$] library (Hochberg et al. 2003) was randomly sampled in the proportion of algae : coral : sand dictated by *BC* for the given site. For example, if $\mathrm{BC_{algae}}$ was 80%, then 80 random algae $R(\lambda)$ were sampled from the library. Community mean $\bar{R}(\lambda)$ was calculated from this weighted sample. Community APAR was calculated as $\int E_d(\lambda;H) \times [1-\bar{R}(\lambda)]\,\mathrm{d}\lambda$.

Finally, fAPAR was calculated as APAR ÷ PAR. The process to calculate fAPAR was repeated 1×10^6 times, and the average result was used as the estimate for further calculation of ε.

Calculating community-scale ε (Objective 1)

Given measured GPP and PAR, as well as model estimates for fAPAR, calculation of ε simply followed Eq. (2).

Estimating ε for algae, coral, and sand (Objective 2)

Given community-scale ε and BC_i, Eq. (4) suggests that a series of linear equations can be used to solve for ε_i:

$$\varepsilon_{\mathrm{community}} = \mathrm{BC_{algae}} \times \varepsilon_{\mathrm{algae}} + \mathrm{BC_{coral}} \times \varepsilon_{\mathrm{coral}} + \mathrm{BC_{sand}} \times \varepsilon_{\mathrm{sand}} \quad (6)$$

Nonnegative least squares with bootstrapping (1×10^6 times) was utilized to estimate probability distributions for each ε_i.

Results

Community-scale ε

With respect to BC, GPP tends to be higher for coral-rich communities, slightly lower for algae-rich communities, and lowest for sand communities (Fig. 2a). However, there are several exceptions to that trend. Lowest GPP is ~ 0.025 mol C m^{-2} d^{-1} for a community with 79% algae. Highest GPP is ~ 1.6 mol C m^{-2} d^{-1} for a community with 73% coral.

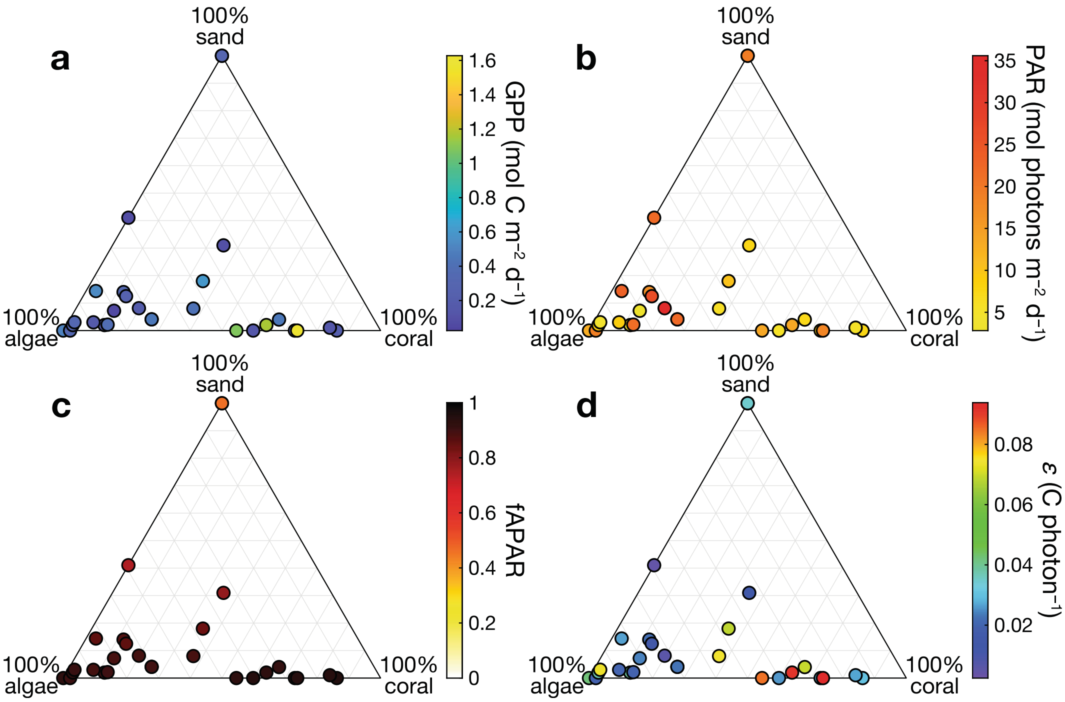

Fig. 2. Ternary plots illustrating results in the context of benthic community structure: the proportional cover of algae, coral, and sand. (**a**) GPP. (**b**) PAR. (**c**) fAPAR. (**d**) Community light-use efficiency. Data are provided in Supporting Information Table S1.

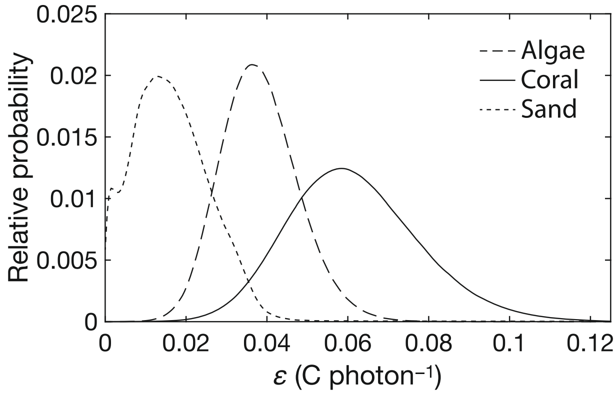

Fig. 3. Relative probability distributions for light-use efficiency of algae, coral, and sand.

There are no apparent trends of PAR with respect to BC (Fig. 2b). This is to be expected, since community composition has no meaningful effect on incident irradiance (multiple scattering and reflection are not significant; Maritorena et al. 1994).

Modeled fAPAR is lowest for sand communities and higher for algae/coral communities (Fig. 2c). Algae and coral communities have roughly equal fAPAR, because their respective $R(\lambda)$ are of the same magnitude (Hochberg et al. 2003). The lowest fAPAR is ~ 0.5 (100% sand), while maximal values are ~ 0.95.

Finally, ε exhibits a clearer trend with respect to BC, with higher values for coral-rich communities and lower values for algae- and sand-rich communities (Fig. 2d). Even still, there are notable exceptions to the trend. The two most coral-rich ($\sim$ 85%) communities have ε of ~ 0.03 C photon^{-1}, while communities with slightly less coral (50–75%) have ε in the range 0.07–0.09 C photon^{-1}. One algae-rich community (94%) has ε of ~ 0.07 C photon^{-1}.

Across all communities, mean ε is 0.040 C photon^{-1}. Considering only those communities where algae or coral are dominant, mean ε is 0.042 C photon^{-1}.

Distributions of ε for algae, coral, and sand

Figure 3 shows relative probability distributions of ε for algae, coral, and sand. Algae has a mean ε of 0.038 C photon^{-1}, and 95% of the distribution falls in the range 0.021–0.058 C photon^{-1}. Coral exhibits a much broader distribution of higher values, with a mean of 0.060 C photon^{-1} and a 95% data range of 0.033–0.097 C photon^{-1}. Sand has a low mean ε of 0.016 C photon^{-1} and a narrow 95% data range of 0.001–0.037 C photon^{-1}.

Discussion

This is the first attempt to estimate light-use efficiency for reef communities based on *absorbed* light (GPP ÷ APAR). This is important because ε represents productive status that is deconvolved from variations in available light and light absorption. Thus, variations in ε are due to other environmental factors. A few prior studies have derived efficiencies based on *available* light (GPP ÷ PAR). Smith (1981) reports an efficiency of 0.038 for an *Acropora* community. Odum and Odum (1955) estimate an efficiency of 0.058 for a largely coral-dominated reef flat at Eniwetak, and Atkinson and Grigg (1984) give an average value of 0.016 for the coralline algal-dominated reef flats of French Frigate Shoals. Assuming an fAPAR of 0.85, these values become 0.045, 0.068, and 0.0188, respectively, which agree well with ε determined in this study.

Mean community ε from this study (0.042 C photon^{-1}) is slightly higher than that derived from the initial slopes of traditional photosynthesis–irradiance curves (often termed quantum yield, 0.032 C photon^{-1}; Hochberg and Atkinson 2008). In theory, the difference may be important: Quantum yield refers to instantaneous photosynthesis, while ε is time-integrated efficiency (Sawall and Hochberg 2018). In fact, for the same plant or community, quantum yield is expected to be higher than ε, since quantum yield represents the unsaturated, steeper portion of the photosynthesis–irradiance curve (Chalker 1981). ε, on the other hand, integrates the entire curve over an extended duration of both unsaturating and saturating irradiances (Sawall and Hochberg 2018), which effectively reduces the slope. In practice, it may not be reasonable to make the comparison presented here. While Hochberg and Atkinson (2008) collated a fairly extensive data set from the literature, the mean value here is for a small collection of sites.

Methodological issues may contribute to the variability observed here. Measurements of underwater PAR are fairly routine and accurate. However, some values here are extrapolated under the assumption of an average reef water clarity, which may lead to deviations from actual PAR. Also, there may be inaccuracies in determination of GPP using the gradient flux approach, which relied on measurements from four separate instruments (two dissolved oxygen sensors, two acoustic Doppler velocimeters) working in tandem (McGillis et al. 2011; Pisapia et al. 2021). Though rigorous intercalibration was performed, there is a possibility of drift or other errors. Importantly, the specific physical environment and dissolved oxygen gradient of a benthic community can impact calculated GPP (Coogan et al. 2022). While best practices were utilized during CORAL for deployment and subsequent calculations—in fact, data for several sites were discarded because measurement conditions did not meet requirements—it is possible that some variability in the final GPP data is due to suboptimal placement of sensors. That would translate to commensurate variability in ε.

Regardless of possible instrument or physical errors, the values for GPP used here are likely underestimates. The method employed by Pisapia et al. (2021) to derive GPP integrates net community production from sunrise to sunset, then adds the average of nighttime respiration (scaled to day length). This approach does not account for differences between rates of light and dark respiration. Light respiration is higher than dark respiration in corals (Kühl et al. 1995;

Schrameyer et al. 2014) and in at least some algae (Comeau et al. 2017). It stands to reason that community-scale respiration would also be higher in the day than at night. However, there is no simple approach to measure community daytime respiration, and nighttime values are the best available means to calculate GPP. As Falter et al. (2011) point out, this approach is consistent with virtually all studies of reef community metabolism since the 1950s and thus provides an unbiased comparison with values in the literature. If higher daytime respiration rates were to be used, the values for GPP reported by Pisapia et al. (2021) would be higher, leading to higher estimates of ε in this study.

Another potential methodological issue contributing to variability in ε is determination of fAPAR. In this study, that parameter is modeled based on a spectral library. The BFTs each exhibit $R(\lambda)$ that is globally conservative with respect to spectral shape, but there is within-class variability with respect to spectral magnitude/brightness (Hochberg et al. 2003, 2004). The fAPAR modeled here for a given BC is an expectation value that could deviate from actual fAPAR for the specific reef community. Thus, an important improvement to more accurate determination of ε would be direct in-water measurement of fAPAR. Such observations should include not only the "foreground" macroscopic corals and algae, but also the "background" algal turfs, sediment pockets, and so on. That is, fAPAR needs to describe the same, complete ecological community for which GPP is measured.

This study considers GPP and ε at the community ($\sim 100\ m^2$) and day+ scales, but ecological processes occur across a hierarchy of scales in both space and time (Hatcher 1997). Light capture and photosynthesis actually operate at the molecular level and at time scales of ms. These processes scale across thylakoid membranes, chloroplasts, cells, algal thalli or coral polyps, to fully differentiated macroalgae or coral colonies. At each level, different factors influence light availability. Up to the cell level, absorption and photosynthesis are strongly influenced by pigment density and pigment packaging (Dubinsky and Falkowski 2011). Within algal thalli or coral polyps, microhabitats (e.g., corallite structures) add further geometric complexity (Enríquez et al. 2005; Wangpraseurt et al. 2014). Habitat composition and topography affect light capture and photosynthesis at the organism scale (Hedley and Enríquez 2010; Wangpraseurt et al. 2014). It is important to note that each higher level of organization integrates the processes across all lower levels. Thus, community GPP and ε integrate those processes across all photosynthetic organisms that comprise the community, which is useful—if not essential—to understand reef function at the system scale (Kinsey 1985; Hatcher 1997).

The light-use efficiency model can conceivably be applied at any level where light absorption and photosynthesis can be measured. However, the method for determination of available light would probably need to vary between scales. For a corallite (0.001–0.01 m), surfaces are as likely to be vertical as horizontal, and surface normals are distributed across the upper hemisphere (Fig. 4a). For a boulder-shaped coral colony (0.01–1 m), the situation is similar, though surface normals are mostly distributed within 60° of zenith (Fig. 4b). A reef community (0.1–10 m) is oriented much more horizontally, and surface normals are mostly within 30° of zenith (Fig. 4c). Finally, a barrier reef and adjacent lagoon (10–1000 m) are virtually flat, with surface normals all near zenith (Fig. 4d). The implication is that, at smaller scales, measurements of incoming light flux should account for complex distributions engendered by microhabitats; the best choice would be a scalar irradiance probe. At larger scales, the incoming light flux is almost entirely downward, and it is sufficient to utilize a cosine corrected plane irradiance probe to quantify light entering the system.

Many reef communities are both biologically and structurally complex. For example, algal turfs may comprise > 100 species mixing at the cm scale (Berner 1990), and coral colonies of various species can co-occur at scales of cm to m (Stoddart 1969). Light-use efficiency may vary both between and within all of these species. Further, they occupy a heterogeneous, three-dimensional seascape, with various taxa preferring different microhabitats (Edmunds et al. 2004). The different taxa are likely to photoacclimate to their respective light environments (Falkowski and Dubinsky 1981), resulting in different organism-scale efficiencies. It is important to note that the community-scale GPP and ε reported here integrate all the constituents of the community at the time of measurement. The derived ε for BFTs is a statistical latent variable that represents the theoretical average for the different BFTs.

Clearly, reef communities have variable ε, depending at least partially on their compositions of BFTs. There may also be variation within the BFTs, for example, between massive, encrusting, and branching coral forms. It is very possible that different algal groups—chlorophytes, phaeophytes, rhodophytes—possess different ε (Hochberg and Atkinson 2008), owing to their different ecological strategies. Exploration of these possible variations, and whether there are predictable trends, is very important to further refine and improve this light-based model.

It is environmental drivers of variability in ε that are of ecological interest. It is likely that community-scale variability is controlled mostly by the ambient light field to which the community is acclimated, for example, ε varies with depth, which has been demonstrated at the organism scale (Hochberg and Atkinson 2008). More generally, for a photosynthetic organism or community, limitation of resources or physical stress lead to increased cost of resource acquisition, which in turn drives optimization of resource allocation (Field 1991). The result is that carbon fixation does not occur at biochemical capacity, but at some level below that capacity. That is, under stress conditions, light-use efficiency is not at its maximal value ε_{max}, but at some reduced value ε (Goetz and Prince 1999). Kinsey (1985) suggests that coral reef GPP can (should) be monitored to detect changes in reef function, which would indicate stress. Monitoring ε

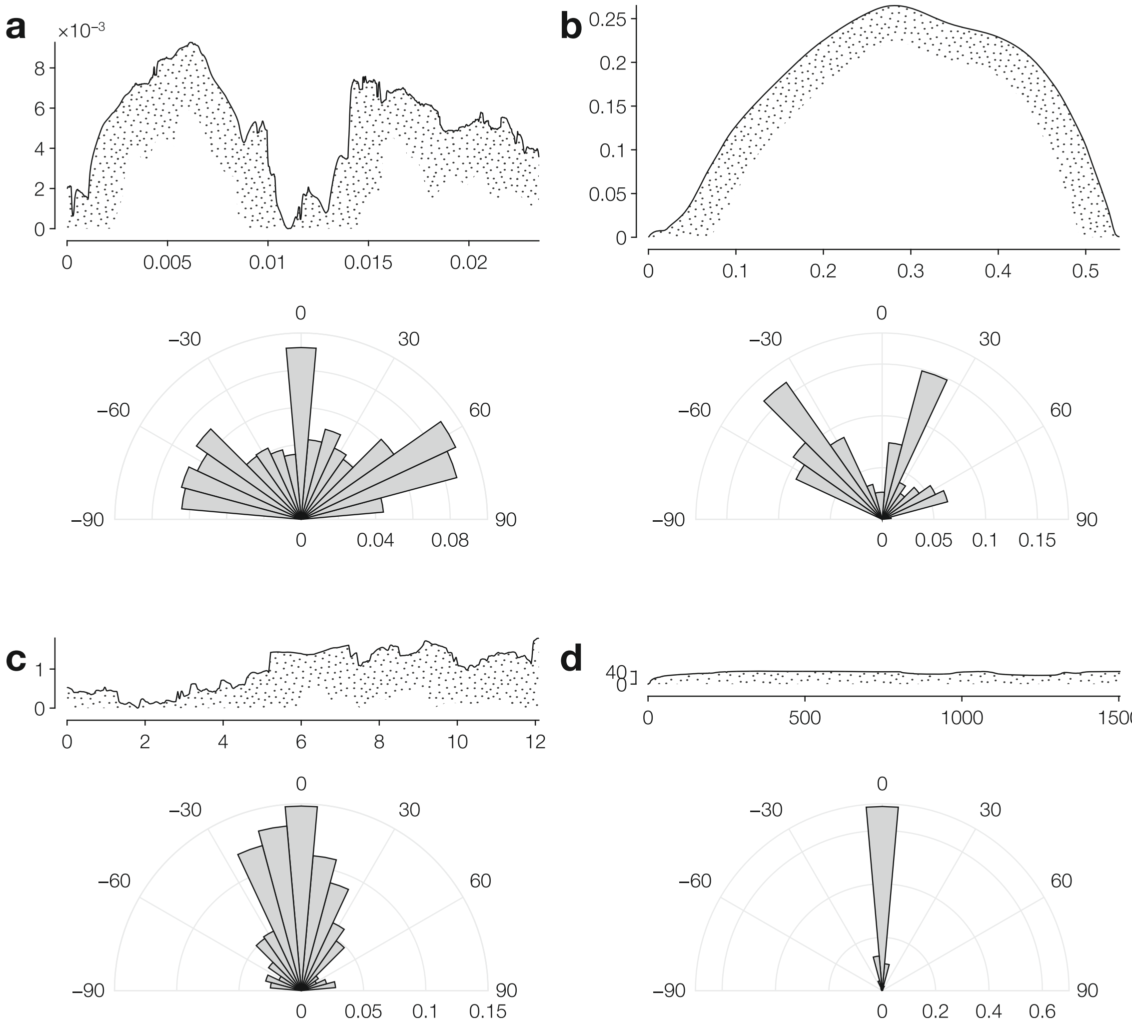

Fig. 4. Cross sections and distributions of corresponding surface normals for reef components at different spatial scales. (**a**) Corallite of *Isophyllia sinuosa* in Bermuda. (**b**) Colony of *Porites lutea* in Palau. (**c**) Fore-reef community in Palau. (**d**) Northern barrier reef and lagoon of Cocos Lagoon, Guam. Three-dimensional data in (**a–c**) derived via photogrammetry. Data in (**d**) measured via airborne lidar (2020 NOAA NGS Topobathy Lidar). Scales for all cross sections have units of m.

might be more useful, because ε normalizes for variations in light. Such monitoring is common for estimating carbon uptake in terrestrial systems (Hilker et al. 2008). For reefs, it would be important to identify trends of ε with respect to the important ecological drivers: temperature, salinity, water flow, prevailing light field, and nutrient availability, among others.

It has been observed in terrestrial plants that different functional types have similar ε (Goetz and Prince 1999). This suggests that any type of resource shortage or stress leads to similar adjustment in biochemical capacity for CO_2 fixation (Field 1991). In turn, this adjustment in photosynthetic machinery causes adjustment of light capture, that is, pigmentation. Thus, light capture integrates both resource status and biochemical capacity for CO_2 assimilation. Inversely, the amount of photosynthetically available radiation absorbed (APAR) by the plant or community measures biological investment in light capture. This points to the possibility for optical measurements of ε. In fact, Eq. (2) directly states that ε is a function of absorptance (fAPAR). Gamon et al. (1992, 1997) have utilized this relationship to develop the "physiological reflectance index," which is an optical index derived from $R(\lambda)$ ($= 1 -$ spectral absorptance), and which can be used as an indicator of ε across terrestrial plant species and functional types. This concept has led to a top-down approach for remote sensing of productivity without the use of field measurements to provide global and regional metabolic estimates for terrestrial systems (Goetz et al. 1999). It is straightforward to envision a similar optical tool that can be applied to coral reef BFTs and communities. The ultimate application would be routine satellite-based observations of reef ε across local, regional, and global scales.

This study presents the best available data describing ε for whole reef communities and for key BFTs. Average community ε is ~ 0.04 C photon^{-1}, which is the same value as for algae. Coral has a higher mean ε at ~ 0.06 C photon^{-1}, and sand has a lower value of ~ 0.02 C photon^{-1}. These values, or their probability distributions, can be applied to introduce light-driven variability into census-based estimates of reef-scale productivity. Ultimately, ε itself can be targeted for in-water and satellite-based monitoring of reef productive status.

Data availability statement

The CORAL data are publicly available in NASA's SeaWiFS Bio-optical Archive and Storage System (SeaBASS), with DOI 10.5067/SeaBASS/CORAL/DATA001. GPP and PAR data reside at https://seabass.gsfc.nasa.gov/archive/CSUN/Carpenter/CORAL/. BC data reside at https://seabass.gsfc.nasa.gov/archive/BIOS/Hochberg/CORAL/. All calculated values are provided as Supporting Information.

References

Andréfouët, S., and C. Payri. 2000. Scaling-up carbon and carbonate metabolism of coral reefs using in-situ data and remote sensing. Coral Reefs **19**: 259–269. doi:10.1007/s003380000117

Atkinson, M. J., and P. Cuet. 2008. Possible effects of ocean acidification on coral reef biogeochemistry: Topics for research. Mar. Ecol. Prog. Ser. **373**: 249–256. doi:10.3354/meps07867

Atkinson, M. J., and J. L. Falter. 2003. Coral reefs, p. 40–64. *In* K. P. Black and G. B. Shimmield [eds.], Biogeochemistry of marine systems. Blackwell/CRC Press. doi:10.1201/9780367812423-2

Atkinson, M. J., and R. W. Grigg. 1984. Model of coral reef ecosystem. II. Gross and net benthic primary production at French Frigate Shoals, Hawaii. Coral Reefs **3**: 13–22. doi:10.1007/bf00306136

Attard, K. M., and R. N. Glud. 2020. Estimating light-use efficiency of benthic habitats using underwater O_2 eddy covariance. Biogeosciences **17**: 4343–4353. doi:10.5194/bg-17-4343-2020

Barnes, D., and M. Devereux. 1984. Productivity and calcification on a coral reef: A survey using pH and oxygen electrode techniques. J. Exp. Mar. Biol. Ecol. **79**: 213–231. doi:10.1016/0022-0981(84)90196-5

Berner, T. 1990. Coral-reef algae, p. 253–264. *In* Z. Dubinsky [ed.], Ecosystems of the world 25: Coral reefs. Elsevier.

Brock, J. C., K. K. Yates, R. B. Halley, I. B. Kuffner, C. W. Wright, and B. G. Hatcher. 2006. Northern Florida reef tract benthic metabolism scaled by remote sensing. Mar. Ecol. Prog. Ser. **312**: 123–139. doi:10.3354/meps312123

Chalker, B. E. 1981. Simulating light-saturation curves for photosynthesis and calcification by reef-building corals. Mar. Biol. **63**: 135–141. doi:10.1007/bf00406821

Comeau, S., R. Carpenter, and P. Edmunds. 2017. Effects of pCO_2 on photosynthesis and respiration of tropical scleractinian corals and calcified algae. ICES J. Mar. Sci. **74**: 1092–1102. doi:10.1093/icesjms/fsv267

Coogan, J., J. E. Rheuban, and M. H. Long. 2022. Evaluating benthic flux measurements from a gradient flux system. Limnol. Oceanogr. Methods **20**: 222–232. doi:10.1002/lom3.10482

Courtney, T. A., and others. 2016. Comparing chemistry and census-based estimates of net ecosystem calcification on a rim reef in Bermuda. Front. Mar. Sci. **3**: 181. doi:10.3389/fmars.2016.00181

Dubinsky, Z., and P. Falkowski. 2011. Light as a source of information and energy in zooxanthellate corals, p. 107–118. In Z. Dubinsky and N. Stambler [eds.], Coral reefs: An ecosystem in transition. Springer. doi:10.1007/978-94-007-0114-4_8

Edmunds, P. J., J. F. Bruno, and D. B. Carlon. 2004. Effects of depth and microhabitat on growth and survivorship of juvenile corals in the Florida Keys. Mar. Ecol. Prog. Ser. **278**: 115–124. doi:10.3354/meps278115

Enríquez, S., E. R. Méndez, and R. Iglesias-Prieto. 2005. Multiple scattering on coral skeletons enhances light absorption by symbiotic algae. Limnol. Oceanogr. **50**: 1025–1032. doi:10.4319/lo.2005.50.4.1025

Falkowski, P. G., and Z. Dubinsky. 1981. Light-shade adaptation of *Stylophora pistillata*, a hermatypic coral from the Gulf of Eilat. Nature **289**: 172–174. doi:10.1038/289172a0

Falter, J. L., M. J. Atkinson, D. W. Schar, R. J. Lowe, and S. G. Monismith. 2011. Short-term coherency between gross primary production and community respiration in an algal-dominated reef flat. Coral Reefs **30**: 53–58. doi:10.1007/s00338-010-0671-9

Falter, J. L., R. J. Lowe, M. J. Atkinson, S. G. Monismith, and D. W. Schar. 2008. Continuous measurements of net production over a shallow reef community using a modified Eulerian approach. J. Geophys. Res. Oceans **113**. doi:10.1029/2007jc004663

Fensholt, R., I. Sandholt, M. S. Rasmussen, S. Stisen, and A. Diouf. 2006. Evaluation of satellite based primary production modelling in the semi-arid Sahel. Remote Sens. Environ. **105**: 173–188. doi:10.1016/j.rse.2006.06.011

Field, C. B. 1991. Ecological scaling of carbon gain to stress and resource availability, p. 35–65. *In* H. A. Mooney, W. E. Winner, and E. J. Pell [eds.], Response of plants to multiple stresses. Academic Press. doi:10.1016/b978-0-08-092483-0.50007-4

Gamon, J. A., J. Penuelas, and C. B. Field. 1992. A narrow-waveband spectral index that tracks diurnal changes in photosynthetic efficiency. Remote Sens. Environ. **41**: 35–44. doi:10.1016/0034-4257(92)90059-s

Gamon, J. A., L. Serrano, and J. S. Surfus. 1997. The photochemical reflectance index: An optical indicator of photosynthetic radiation use efficiency across species, functional types, and nutrient levels. Oecologia **112**: 492–501. doi:10.1007/s004420050337

Gattuso, J.-P., D. Allemand, and M. Frankignoulle. 1999. Photosynthesis and calcification at cellular, organismal, and community levels in coral reefs: A review of interactions and control by carbonate chemistry. Am. Zool. **39**: 160–183. doi:10.1093/icb/39.1.160

Gitelson, A. A., and J. A. Gamon. 2015. The need for a common basis for defining light-use efficiency: Implications for productivity estimation. Remote Sens. Environ. **156**: 196–201. doi:10.1016/j.rse.2014.09.017

Goetz, S. J., and S. D. Prince. 1999. Modelling terrestrial carbon exchange and storage: Evidence and implications of functional convergence in light-use efficiency. Adv. Ecol. Res. **28**: 57–92. doi:10.1016/s0065-2504(08)60029-x

Goetz, S. J., S. D. Prince, S. N. Goward, M. M. Thawley, and J. Small. 1999. Satellite remote sensing of primary production: An improved production efficiency modeling approach. Ecol. Model. **122**: 239–255. doi:10.1016/s0304-3800(99)00140-4

Gregg, W. W., and K. L. Carder. 1990. A simple spectral solar irradiance model for cloudless maritime atmospheres. Limnol. Oceanogr. **35**: 1657–1675. doi:10.4319/lo.1990.35.8.1657

Grigg, R. W., J. J. Polovina, and M. J. Atkinson. 1984. Model of a coral reef ecosystem. III. Resource limitation, community regulation, fisheries yield and resource management. Coral Reefs **3**: 23–27. doi:10.1007/bf00306137

Hatcher, B. G. 1990. Coral reef primary productivity – A hierarchy of pattern and process. Trends Ecol. Evol. **5**: 149–155. doi:10.1016/0169-5347(90)90221-x

Hatcher, B. G. 1997. Coral reef ecosystems: How much greater is the whole than the sum of the parts? Coral Reefs **16**: S77–S91. doi:10.1007/s003380050244

Hedley, J., and S. Enríquez. 2010. Optical properties of canopies of the tropical seagrass *Thalassia testudinum* estimated by a three-dimensional radiative transfer model. Limnol. Oceanogr. **55**: 1537–1550. doi:10.4319/lo.2010.55.4.1537

Heinsch, F. A., and others. 2003. User's guide: GPP and NPP (MOD17A2/A3) products NASA MODIS land algorithm, version 2.0. p. 57. NASA.

Hilker, T., N. C. Coops, M. A. Wulder, T. A. Black, and R. D. Guy. 2008. The use of remote sensing in light use efficiency based models of gross primary production: A review of current status and future requirements. Sci. Total Environ. **404**: 411–423. doi:10.1016/j.scitotenv.2007.11.007

Hochberg, E. J., and M. J. Atkinson. 2008. Coral reef benthic productivity based on optical absorptance and light-use efficiency. Coral Reefs **27**: 49–59. doi:10.1007/s00338-007-0289-8

Hochberg, E. J., M. J. Atkinson, and S. Andréfouët. 2003. Spectral reflectance of coral reef bottom-types worldwide and implications for coral reef remote sensing. Remote Sens. Environ. **85**: 159–173. doi:10.1016/s0034-4257(02)00201-8

Hochberg, E. J., M. J. Atkinson, A. Apprill, and S. Andréfouët. 2004. Spectral reflectance of coral. Coral Reefs **23**: 84–95. doi:10.1007/s00338-003-0350-1

Hochberg, E. J., S. A. Peltier, and S. Maritorena. 2020. Trends and variability in spectral diffuse attenuation of coral reef waters. Coral Reefs **39**: 1377–1389. doi:10.1007/s00338-020-01971-1

Kinsey, D. W. 1978. Productivity and calcification estimates using slack-water periods and field enclosures, p. 439–468. *In* D. R. Stoddart and R. E. Johannes [eds.], Coral reefs: Research methods. UNESCO.

Kinsey, D. W. 1979. Carbon turnover and accumulation by coral reefs. Univ. of Hawaii at Manoa.

Kinsey, D. W. 1983. Standards of performance in coral reef primary production and carbon turnover. Perspectives on coral reefs. Brian Clouston Publisher, p. 209–220.

Kinsey, D. W. 1985. Metabolism, calcification and carbon production I: Systems level studies. Fifth International Coral Reef Congress, p. 505–526.

Kühl, M., Y. Cohen, T. Dalsgaard, B. B. Jørgensen, and N. P. Revsbech. 1995. Microenvironment and photosynthesis of zooxanthellae in scleractinian corals studied with microsensors for O_2, pH and light. Mar. Ecol. Prog. Ser. **117**: 159–172.

Long, M. H., P. Berg, D. de Beer, and J. C. Zieman. 2013. In situ coral reef oxygen metabolism: An eddy correlation study. PLoS One **8**: e58581. doi:10.1371/journal.pone.0058581

Maritorena, S., A. Morel, and B. Gentili. 1994. Diffuse reflectance of oceanic shallow waters: Influence of water depth and bottom albedo. Limnol. Oceanogr. **39**: 1689–1703. doi:10.4319/lo.1994.39.7.1689

Marsh, J. A., and S. V. Smith. 1978. Productivity measurements of coral reefs in flowing water, p. 361–377. *In* D. R. Stoddart and R. E. Johannes [eds.], Coral reefs: Research methods. UNESCO.

McGillis, W. R., C. Langdon, B. Loose, K. Yates, and J. Corredor. 2011. Productivity of a coral reef using boundary layer and enclosure methods. Geophys. Res. Lett. **38**. doi:10.1029/2010gl046179

Monteith, J. 1972. Solar radiation and productivity in tropical ecosystems. J. Appl. Ecol. **9**: 747–766. doi:10.2307/2401901

Monteith, J. L. 1977. Climate and the efficiency of crop production in Britain. Philos. Trans. R Soc. Lond. B Biol. Sci. **281**: 277–294. doi:10.1098/rstb.1977.0140

Morel, A. 1978. Available, usable and stored radiant energy in relation to marine photosynthesis. Deep Sea Res. **25**: 673–688. doi:10.1016/0146-6291(78)90623-9

Moses, C. S., S. Andréfouët, C. J. Kranenburg, and F. E. Muller-Karger. 2009. Regional estimates of reef carbonate dynamics and productivity using Landsat 7 ETM+, and potential impacts from ocean acidification. Mar. Ecol. Prog. Ser. **380**: 103–115. doi:10.3354/meps07920

Odum, H. T., and E. P. Odum. 1955. Trophic structure and productivity of a windward reef community on Eniwetok Atoll. Ecol. Monogr. **25**: 291–320. doi:10.2307/1943285

Pisapia, C., E. J. Hochberg, and R. Carpenter. 2021. Modes of metabolic performance of Pacific reefs. Geophys. Res. Lett. **48**: e2021GL092930. doi:10.1029/2021gl092930

Platt, T. 1986. Primary production of the ocean water column as a function of surface light intensity: Algorithms for remote sensing. Deep Sea Res. **33**: 149–163. doi:10.1016/0198-0149(86)90115-9

Polovina, J. J. 1984. Model of a coral reef ecosystem. I. The ECOPATH model and its application to French Frigate Shoals. Coral Reefs **3**: 1–11. doi:10.1007/bf00306135

Running, S. W., R. R. Nemani, F. A. Heinsch, M. S. Zhao, M. Reeves, and H. Hashimoto. 2004. A continuous satellite-derived measure of global terrestrial primary production. Bioscience **54**: 547–560 doi:10.1641/0006-3568(2004)054%5B0547:ACSMOG%5D2.0.CO;2

Sawall, Y., and E. J. Hochberg. 2018. Diel versus time-integrated (daily) photosynthesis and irradiance relationships of coral reef organisms and communities. PLoS One **13**: e0208607. doi:10.1371/journal.pone.0208607

Schrameyer, V., D. Wangpraseurt, R. Hill, M. Kühl, A. W. Larkum, and P. J. Ralph. 2014. Light respiratory processes and gross photosynthesis in two scleractinian corals. PLoS One **9**: e110814. doi:10.1371/journal.pone.0110814

Sims, D. A., and others. 2006. On the use of MODIS EVI to assess gross primary productivity of north American ecosystems. J. Geophys. Res. Biogeosci. **111**. doi:10.1029/2006jg000162

Smith, S. V. 1981. The Houtman Abrolhos Islands—Carbon metabolism of coral reefs at high-latitude. Limnol. Oceanogr. **26**: 612–621. doi:10.4319/lo.1981.26.4.0612

Stoddart, D. R. 1969. Ecology and morphology of recent coral reefs. Biol. Rev. Camb. Philos. Soc. **44**: 433–498. doi:10.1111/j.1469-185X.1969.tb00609.x

Takeshita, Y., T. Cyronak, T. R. Martz, T. Kindeberg, and A. J. Andersson. 2018. Coral reef carbonate chemistry variability at different functional scales. Front. Mar. Sci. **5**: 175. doi:10.3389/fmars.2018.00175

Takeshita, Y., and others. 2016. Assessment of net community production and calcification of a coral reef using a boundary layer approach. J. Geophys. Res. Oceans **121**: 5655–5671. doi:10.1002/2016jc011886

Wangpraseurt, D., and others. 2014. The in situ light microenvironment of corals. Limnol. Oceanogr. **59**: 917–926. doi:10.4319/lo.2014.59.3.0917

Wyman, K., Z. Dubinsky, J. Porter, and P. Falkowski. 1987. Light absorption and utilization among hermatypic corals: A study in Jamaica, West Indies. Mar. Biol. **96**: 283–292. doi:10.1007/bf00427028

Yates, K. K., and R. B. Halley. 2003. Measuring coral reef community metabolism using new benthic chamber technology. Coral Reefs **22**: 247–255. doi:10.1007/s00338-003-0314-5

Acknowledgments

This material is based in part upon work supported by NASA Awards NNX-16AB05G, 80NSSC21K1159, and 80NSSC21K0603 to EJH.

Conflict of Interest

The authors declare no conflicts of interest.

Submitted 19 August 2023
Revised 18 December 2023
Accepted 16 January 2024

Associate editor: David Antoine